

## Structural and electro-optic properties of laser ablated $\text{Bi}_4\text{Ti}_3\text{O}_{12}$ thin films on $\text{SrTiO}_3(100)$ and $\text{SrTiO}_3(110)$

W. Jo, G-C. Yi, T. W. Noh, D-K. Ko, Y. S. Cho, and S-I. Kwun

Citation: [Applied Physics Letters](#) **61**, 1516 (1992); doi: 10.1063/1.107534

View online: <http://dx.doi.org/10.1063/1.107534>

View Table of Contents: <http://scitation.aip.org/content/aip/journal/apl/61/13?ver=pdfcov>

Published by the [AIP Publishing](#)

---

### Articles you may be interested in

[Structural and electro-optic properties of  \$\text{Ba}\_{0.7}\text{Sr}\_{0.3}\text{TiO}\_3\$  thin films grown on various substrates using pulsed laser deposition](#)

[J. Appl. Phys.](#) **101**, 043515 (2007); 10.1063/1.2646014

[BaTiO<sub>3</sub> – SrTiO<sub>3</sub> multilayer thin film electro-optic waveguide modulator](#)

[Appl. Phys. Lett.](#) **89**, 242904 (2006); 10.1063/1.2404982

[La-doped effect on the ferroelectric properties of  \$\text{Bi}\_4\text{Ti}\_3\text{O}\_{12}\$  –  \$\text{SrBi}\_4\text{Ti}\_4\text{O}\_{15}\$  thin film fabricated by pulsed laser deposition](#)

[J. Appl. Phys.](#) **92**, 5420 (2002); 10.1063/1.1510557

[Structural and electro-optic properties of pulsed laser deposited  \$\text{Bi}\_4\text{Ti}\_3\text{O}\_{12}\$  thin films on MgO](#)

[Appl. Phys. Lett.](#) **63**, 2198 (1993); 10.1063/1.110552

[Structural and optical properties of ferroelectric  \$\text{Bi}\_4\text{Ti}\_3\text{O}\_{12}\$  thin films by sol-gel technique](#)

[Appl. Phys. Lett.](#) **59**, 2389 (1991); 10.1063/1.106025

---



# Structural and electro-optic properties of laser ablated $\text{Bi}_4\text{Ti}_3\text{O}_{12}$ thin films on $\text{SrTiO}_3(100)$ and $\text{SrTiO}_3(110)$

W. Jo, G.-C. Yi, T. W. Noh, D.-K. Ko, Y. S. Cho, and S.-I. Kwun  
Department of Physics, Seoul National University, 151-742, Seoul, Korea

(Received 6 April 1992; accepted for publication 20 July 1992)

$\text{Bi}_4\text{Ti}_3\text{O}_{12}$  thin films have been grown by laser ablation on  $\text{SrTiO}_3(100)$  and  $\text{SrTiO}_3(110)$  substrates. Substrate surface orientation is found to be an important growth parameter which determines crystal axis orientation, grain growth behavior, and electro-optic properties of the  $\text{Bi}_4\text{Ti}_3\text{O}_{12}$  thin films. The films grown on  $\text{SrTiO}_3(110)$  shows a ferroelectric phase transition near  $720^\circ\text{C}$  and a large quadratic electro-optic effect with the effective coefficient  $1.1 \times 10^{-16} \text{ m}^2/\text{V}^2$ .

$\text{Bi}_4\text{Ti}_3\text{O}_{12}$  is an interesting ferroelectric material with useful properties for nonvolatile memory, piezoelectric, and electro-optic devices.<sup>1</sup> Recently, epitaxial  $\text{Bi}_4\text{Ti}_3\text{O}_{12}$  thin films have been successfully grown by pulsed excimer laser deposition on  $\text{SrTiO}_3(100)$ ,<sup>2</sup>  $\text{MgO}(110)$ ,<sup>3</sup> and  $\text{YBa}_2\text{Cu}_3\text{O}_7(001)$ .<sup>4</sup> The feasibility for growing lattice-matched heterostructures makes this material very attractive for several applications. In this letter we report effects of substrate surface orientation, i.e., (100) and (110) faces of  $\text{SrTiO}_3$  single crystal, on structural and electro-optic properties of the laser ablated  $\text{Bi}_4\text{Ti}_3\text{O}_{12}$  films.

A visible laser, i.e., second harmonics (532 nm) of a Q-switched Nd:YAG laser, was used in this study instead of commonly used ultraviolet lasers.<sup>2-4</sup> The laser was pulsed at a rate of 20 Hz, and the beam was focused with a quartz lens onto a polycrystalline, single-phase  $\text{Bi}_4\text{Ti}_3\text{O}_{12}$  target. Fluence of the beam on the target was estimated to be  $1.5\text{--}2 \text{ J/cm}^2$ . Thin-film deposition was carried on a single-crystal substrate,  $\text{SrTiO}_3(100)$  or  $\text{SrTiO}_3(110)$ , which was maintained at temperature of  $730\text{--}750^\circ\text{C}$  in oxygen atmosphere of 200 mTorr. After the deposition, the thin films were *in situ* annealed at  $500^\circ\text{C}$  in oxygen atmosphere of 500 Torr for 30 min. They were characterized using x-ray diffractometry methods ( $2\theta$  scan, rocking curve, and x-ray pole figure) and scanning electron microscopy (SEM). Their linear birefringences were also measured as a function of temperature and dc electric field.

X-ray diffraction patterns are shown in Fig. 1. The pattern of the  $\text{Bi}_4\text{Ti}_3\text{O}_{12}$  thin film on  $\text{SrTiO}_3(100)$ , as shown in Fig. 1(a), has only (00 $l$ ) peaks in agreement with an earlier report.<sup>2</sup> The rocking curve full width at half maximum (FWHM) is about  $0.3^\circ$  for the (006) peak of the film. This value informs us that grains are well aligned with their  $c$ -axes normal to the substrate. However, the film on  $\text{SrTiO}_3(110)$  shows a (117) peak as well as (00 $l$ ) peaks, as shown in Fig. 1(b). This result indicates that this film is composed of grains with more than one orientation.

A relation between the crystal axes of  $\text{Bi}_4\text{Ti}_3\text{O}_{12}$  and the in-plane vectors of  $\text{SrTiO}_3$  can be obtained using x-ray pole figure. The Schultz geometry<sup>5</sup> was used in this measurement. The  $\alpha$  and  $\beta$  rotations are coupled so that a  $360^\circ$  rotation of  $\beta$  corresponds to a  $2.5^\circ$  decrease of  $\alpha$ . (The  $2\theta$  scan corresponds to  $\alpha=90^\circ$ .) As shown in Fig. 2(a), the four (117) reflections of the film on  $\text{SrTiO}_3(100)$  are lo-

cated at  $\beta=0^\circ, 90^\circ, 180^\circ$ , and  $270^\circ$  with  $\alpha \cong 40^\circ$ . This indicates that the [117] direction of the  $\text{Bi}_4\text{Ti}_3\text{O}_{12}$  grains is aligned in the  $ac$ -plane of  $\text{SrTiO}_3$  lattice with the polar angle of about  $50^\circ$  from the  $c$ -axis of the substrate. This epitaxial growth behavior can be understood from the fact that the lattice constants of  $\text{Bi}_4\text{Ti}_3\text{O}_{12}$  ( $a=5.448 \text{ \AA}$  and  $b=5.410 \text{ \AA}$ ) are close to the length of the face diagonal of the  $\text{SrTiO}_3$  lattice ( $a=3.905 \text{ \AA}$  for  $\text{SrTiO}_3$ ).

Figure 2(b) shows a pole figure of the film on  $\text{SrTiO}_3(110)$  for (117) and (008) reflections of  $\text{Bi}_4\text{Ti}_3\text{O}_{12}$ . Similar to Fig. 2(a) the resulting (117) reflections, which come from the grains with their  $c$ -axes normal to the substrate, have fourfold azimuthal orientations along the [100] and [110] directions of the substrate. This tendency can be understood from the fact that the lattice constant of  $\text{SrTiO}_3$  along the [110] direction is very close to that of  $\text{Bi}_4\text{Ti}_3\text{O}_{12}$  along  $a$ -axis. On the other hand, the (008) reflections show strong peaks at  $\beta \cong 20^\circ$  and  $200^\circ$  with  $\alpha \cong 40^\circ\text{--}48^\circ$ . These reflections come from the grains with their (117) planes nearly parallel to the substrate. Most of these grains are

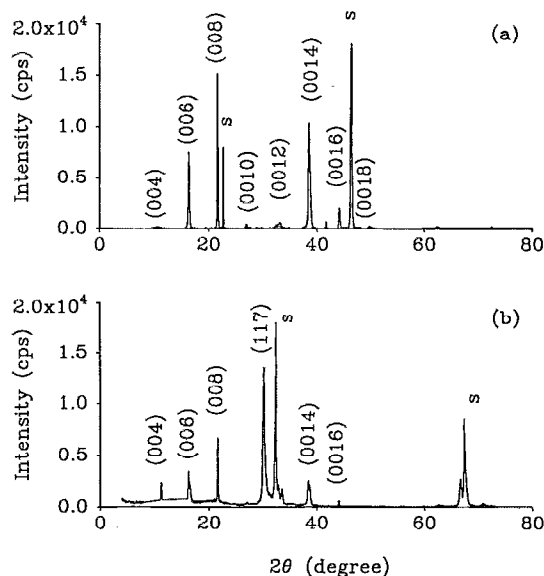


FIG. 1. X-ray diffraction patterns of  $\text{Bi}_4\text{Ti}_3\text{O}_{12}$  thin films on (a)  $\text{SrTiO}_3(100)$  and (b)  $\text{SrTiO}_3(110)$ . The character "s" indicates peaks of  $\text{SrTiO}_3$ .

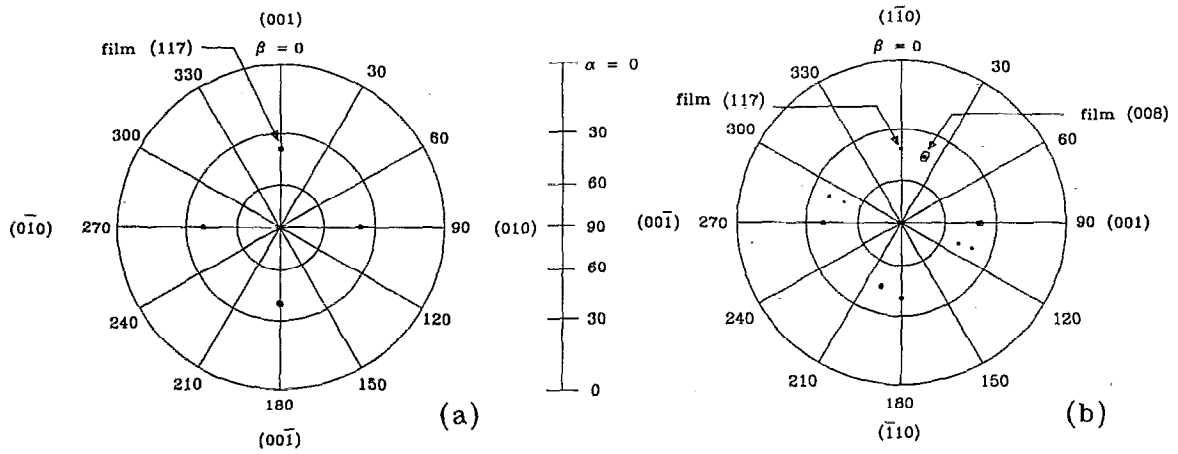


FIG. 2. X-ray pole figures of  $\text{Bi}_4\text{Ti}_3\text{O}_{12}$  thin films on (a)  $\text{SrTiO}_3(100)$  and (b)  $\text{SrTiO}_3(110)$ .

oriented along an angle of  $20^\circ$  from  $[110]$  direction of  $\text{SrTiO}_3$  and an angle around  $46^\circ$  from the normal direction of the  $\text{SrTiO}_3$  substrate. Therefore, the film on  $\text{SrTiO}_3(110)$  is composed of grains which are highly oriented along some directions.

SEM micrographs, shown in Fig. 3, also demonstrate an interesting difference in grain growth behavior between the  $\text{Bi}_4\text{Ti}_3\text{O}_{12}$  thin films. The film on  $\text{SrTiO}_3(100)$  shows grain growth without any preferred habit but the film on  $\text{SrTiO}_3(110)$  shows growth of elliptical grains which are aligned along a direction about  $20^\circ$  away from the  $[110]$  direction of the substrate. This tilt angle is similar to that of the strongest (008) peaks in Fig. 2(b). Therefore, the  $\text{SrTiO}_3$  surface orientation influences grain growth behavior as well as crystal axis orientation.

Linear birefringence,  $\Delta n$ , was measured by the Senarmont method<sup>6</sup> using a 15 mW He-Ne laser. For a thin film of 5000 Å thickness, the resolution of  $\Delta n$  in our system was about  $10^{-4}$ . Birefringence of a blank  $\text{SrTiO}_3$  substrate was

measured separately and showed no significant shift within our experimental error. For the temperature dependence measurement, the samples were heated with a furnace. For the electric field dependence measurement, silver electrodes were thermally evaporated on a thin film with a separation of 0.5 mm. A dc electric field up to 20 kV/cm was applied parallel to the  $[110]$  direction of the  $\text{SrTiO}_3(110)$  substrate. The light enters with its polarization at an angle of  $45^\circ$  with respect to the direction of the electric field.

Figure 4(a) shows the temperature dependent birefringences for the  $\text{Bi}_4\text{Ti}_3\text{O}_{12}$  thin films. The birefringence of the film on  $\text{SrTiO}_3(100)$ ,  $\Delta n_{(100)}$ , is similar to that of a single-crystal  $\text{Bi}_4\text{Ti}_3\text{O}_{12}$  when the light enters the crystal along the  $c$ -axis.<sup>7</sup> The birefringence of the film on  $\text{SrTiO}_3(110)$ ,  $\Delta n_{(110)}$ , is much larger than  $\Delta n_{(100)}$ , and the former comes from the contribution of  $\Delta n$ 's along three

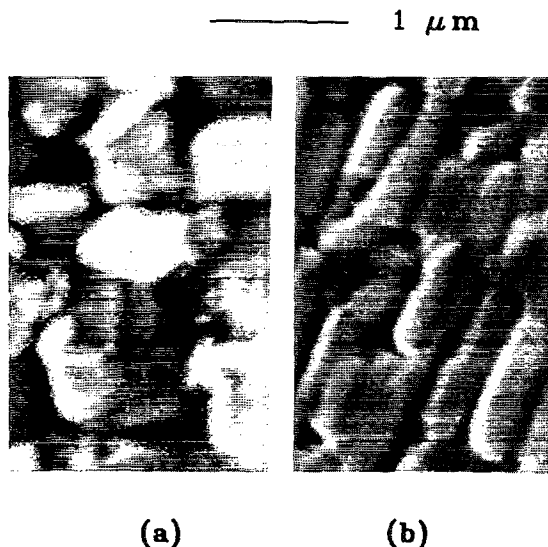


FIG. 3. Scanning electron micrographs of  $\text{Bi}_4\text{Ti}_3\text{O}_{12}$  thin films on (a) on  $\text{SrTiO}_3(100)$  and (b)  $\text{SrTiO}_3(110)$ .

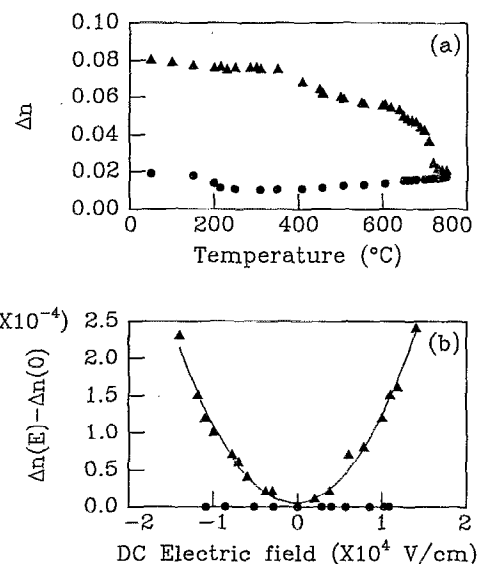


FIG. 4. (a) Temperature dependence of linear birefringence shift,  $\Delta n$ , of  $\text{Bi}_4\text{Ti}_3\text{O}_{12}$  thin films. (b) Changes in  $\Delta n$  as a function of applied electric field. In these figures, solid circles represent the data for the film on  $\text{SrTiO}_3(100)$  and solid triangles represent those on  $\text{SrTiO}_3(110)$ .

crystal axes.<sup>7</sup> An abrupt change in  $\Delta n_{(110)}$ , which is related to the ferroelectric transition, is observed near 720 °C. This Curie temperature is higher than that of a single crystal, i.e., 676 °C.<sup>7</sup> A similar shift of 50 °C in the Curie temperature was reported for the epitaxial  $\text{PbTiO}_3$  thin films,<sup>8</sup> and it was interpreted as a stress induced shift.<sup>9</sup>

Figure 4(b) shows changes in  $\Delta n$ , i.e.,  $\Delta n(E) - \Delta n(E=0)$ , as a function of applied electric field  $E$ . Little changes in  $\Delta n$  are observed for the thin film on  $\text{SrTiO}_3(100)$ . However, the film on  $\text{SrTiO}_3(110)$  shows very large changes in  $\Delta n$  which can be fitted to a quadratic equation of  $E$ . The linear electro-optic component is found to be very small and that is in agreement with the fact that our measured  $\Delta n$ 's are the average responses from the multidomain material.<sup>10</sup> The effective quadratic electro-optic coefficient is calculated to be  $1.1 \times 10^{-16} \text{ m}^2/\text{V}^2$ . This value is larger than those of most ferroelectric films [typically,  $10^{-17}$ – $10^{-19} \text{ m}^2/\text{V}^2$  for  $(\text{Sr},\text{Ba})\text{Nb}_2\text{O}_6$ ,  $\text{BaTiO}_3$ , and  $\text{Ba}_2\text{NaNb}_5\text{O}_{15}$ ],<sup>11</sup> and it is also larger than that of sputtered  $(\text{Pb},\text{La})(\text{Zr},\text{Ti})\text{O}_3$  thin film [i.e.,  $4.43 \times 10^{-17} \text{ m}^2/\text{V}^2$ ] by a factor of 2.<sup>11</sup> Therefore, the  $\text{Bi}_4\text{Ti}_3\text{O}_{12}$  film on  $\text{SrTiO}_3(110)$  is a good candidate material for the electro-optic device applications.

In summary,  $\text{Bi}_4\text{Ti}_3\text{O}_{12}$  thin films have been grown on  $\text{SrTiO}_3(100)$  and  $\text{SrTiO}_3(110)$  by laser ablation. From x-ray diffraction SEM and linear birefringence measurements, it is found that the  $\text{SrTiO}_3$  surface orientation determines crystal axis orientation, grain growth behavior,

and electro-optic properties of the  $\text{Bi}_4\text{Ti}_3\text{O}_{12}$  thin films. A ferroelectric phase transition is observed near 720 °C, which is higher than the transition temperature of a bulk  $\text{Bi}_4\text{Ti}_3\text{O}_{12}$ . The effective quadratic electro-optic coefficient for the film grown on  $\text{SrTiO}_3(110)$  is evaluated to be  $1.1 \times 10^{-16} \text{ m}^2/\text{V}^2$ .

This work is supported by the ADD (Contract No. UD920055BD) and by the KOSEF through the Science Research Center of Excellence Program.

<sup>1</sup>S. Y. Wu, W. J. Takei, and M. H. Francombe, *Ferroelectrics* **10**, 209 (1976).

<sup>2</sup>R. Ramesh, K. Luther, B. Wilkens, D. L. Hart, E. Wang, J. M. Tarascon, A. Inam, X. D. Wu, and T. Venkatesan, *Appl. Phys. Lett.* **57**, 1505 (1990).

<sup>3</sup>H. Buhay, S. Sinharoy, W. H. Kasner, M. H. Francombe, D. R. Lampe, and E. Stepke, *Appl. Phys. Lett.* **58**, 1470 (1991).

<sup>4</sup>R. Ramesh, A. Inam, B. Wilkens, W. K. Chan, T. Sands, D. K. Fork, T. H. Geballe, J. Evans, and J. Bullington, *Appl. Phys. Lett.* **59**, 1782 (1991).

<sup>5</sup>J. F. M. Cillessen, D. M. de Leeuw, A. J. Kinneging, P. C. Zalm, and P. F. Bongers, *J. Appl. Phys.* **68**, 6507 (1990).

<sup>6</sup>K. Nomura and H. Ogawa, *J. Appl. Phys.* **70**, 3234 (1991).

<sup>7</sup>S. E. Cummins and L. E. Cross, *J. Appl. Phys.* **39**, 2268 (1968).

<sup>8</sup>K. Kushida and H. Takeuchi, *Appl. Phys. Lett.* **50**, 1800 (1987); K. Kushida and H. Takeuchi, *Ferroelectrics* **108**, 3 (1990).

<sup>9</sup>G. A. Rossetti, Jr., L. E. Cross, and K. Kushida, *Appl. Phys. Lett.* **59**, 2524 (1991).

<sup>10</sup>T. M. Graettinger, S. H. Rou, M. S. Ameen, O. Auciello, and A. I. Kingon, *Appl. Phys. Lett.* **58**, 1964 (1991).

<sup>11</sup>A. Y. Wu, F. Wang, C.-B. Juang, and C. Bustamante, *Mater. Res. Soc. Symp. Proc.* **200**, 261 (1990).